

# REFOLDING A $\beta$ -BARREL MEMBRANE PROTEIN

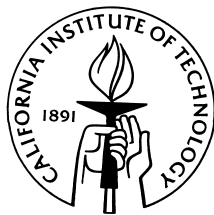
Thesis by

Gitrada Arjara

In Partial Fulfillment of the Requirements

for the Degree of

Doctor of Philosophy



California Institute of Technology

Pasadena, California

2007

(Defended May 25, 2007)

© 2007

Gitrada Arjara

All Rights Reserved

## ACKNOWLEDGEMENTS

I would like to thank to my PhD advisors, Professors Harry Gray and Jack Richards, for supporting me during these past five years. Harry is someone you will instantly love and never forget once you meet him. He's the funniest advisor and one of the smartest people I know. I hope that I could be as lively, enthusiastic, and energetic as Harry and to someday be able to command an audience as well as he can. Jack has been supportive and has given me the freedom to pursue various projects without objection. He has also provided insightful discussions about the research. I am also very grateful to Jay Winkler for his scientific advice and knowledge and many insightful discussions and suggestions. He is my primary resource for getting my science questions answered and was instrumental in helping me crank out this thesis, all in one month. I also have to thank the members of my PhD committee, Professors Doug Rees, Jackie Barton, and Bil Clemons for their helpful career advice and suggestions in general.

I will forever be thankful to my former college research advisor, Professor Catherine Drennan. Cathy has been helpful in providing advice many times during my graduate school career. She was and remains my best role model for a scientist, mentor, and teacher. I still think fondly of my time as an undergraduate student in her lab. Cathy was the reason why I decided to go to pursue a career in research. Her enthusiasm and love for teaching is contagious.

I also thank my OmpA collaborator, Professor Judy Kim (UCSD), for her help and teaching while she was a postdoc in the Gray group. She's a great spectroscopist and has taught the grad student folders a lot about laser spectroscopy. Judy's a good teacher

who encouraged and expected us to think more independently about our experiments and results.

A good support system is important to surviving and staying sane in grad school. I was lucky to be a part of one we like to call “sub-sub” and refer to Melanie Pribisko, Bert Lai, and myself. These two friends formed the core of my research time in the Gray group. I couldn’t have survived Askaban (now called the Red Light District) without them. We’ve all been there for one another and have taught ourselves and each other many tools and issues of protein folding. I know that I could always ask them for advice and opinions on lab related issues. Mel is a wonderful and generous friend who has been through a lot and I admire her positive outlook and her ability to smile despite the situation. I remember first meeting Mel during our Caltech visiting weekend five years ago and we managed to keep in touch during the year that she was working. I’ll never forget the many wonderful lunches and fun activities we’ve done together, including that huge HBG card. Thanks so much for organizing that post-wedding reception for us! In addition to my husband, Melanie was the one who was there for me during the thesis writing hell to help me quickly proofread and give suggestions. I know that when we are old, Melanie will still be there as a supportive and caring friend. Bert, aka O-B!!!! or just BBB!!! is someone you won’t forget. He cares about and will look out for his people. But watch out or else SBW will come out! I know I can count on Bert to always provide helpful suggestions and help with instrumentation and general lab questions. I will miss our silliness and childish sessions like that time we flew first class to San Francisco (my first time in first class! Thanks B!). I still get a laugh when I reminisce about the time sub-sub took a little trip to Rite-aid this past summer.

I thank all the present members of the Gray and Richards group: John Magyar (extremely knowledgeable in just about everything, helpful, and friendly - best of luck at Barnard! Thanks for helping with the prop editing.), Kate Pletneva (has been helpful with answering FET questions and other questions in general, best wishes as you start your career at Dartmouth), Matt Hartings (a nice and helpful person who has been pretty supportive during my search for jobs and writing and will make a good professor soon), Tetsu Kimura (a friendly and knowledgeable expert in protein folding who has also helped me with the laser many times), Keiko Yokoyama (so friendly and I'm glad to have her as a friend) and Lionel Cheruzel (aka Frenchy, the funny and friendly office mate from France). Brian Leigh has been so helpful when I first arrived to Caltech. He was instrumental in helping me through candidacy and I will forever be grateful to him. I'll also not forget his help with moving our refrigerator and use of this good old SUV during the many furniture moves. Best wishes to him as he finishes up.

I also thank the the fun 4<sup>th</sup> year students, Bert, Mel, Don (friendly guy from Louisiana and has the most playful cat), Crystal (the group party planner who organizes the Gray group parties), and the optimistic second years, Jillian (friendly, nice, and smart gal, also from MIT), Kyle (throws fun parties and knows how to make delicious drinks), Gretchen (a friendly and all around great labmate who I'm glad to have with us in the Red Light District), Morgan (always friendly and cheerful about everything). They are all a fun bunch with lots of enthusiasm and optimism and remind me of how I used to be when I first got to Caltech. All the young Gray groupers, Heather, Alec, Charlotte, Paul, and Josh for continuing work in the Gray group. I haven't gotten a chance to get to really know them since I've been in a hole this past year but they've all been so friendly and

personable to me. I wish these younger students the best of luck and hopefully their time in graduate school won't turn them into bitter old farts like me. I'm also glad to have worked with a wonderful undergraduate student, Ekta Bhojwani for a couple of quarters last year. I value her friendship and support as well.

I also thank people who were not part of the Gray group but helped me out, including Bruce Brunshwig (lots of help with DLS use and background), Yuling Sheng (a wonderful person with great lab skills who was nice to have on the azurin project during my second year), and Cora MacBeth and Professor Jonas Peters during my first year here.

I also thank the past members of the Gray/Richard groups: Malin Abrahamsson (a wonderful and friendly person who was instrumental with helping analyze data for azurin and helped train me on the nanosecond laser system), Jeremy Weaver (great office mate who I would go to for answers to many questions), Jeremiah Miller (helped me a lot when I first got to Caltech and taught me basics of synthesis), Katrine Musich (taught me a lot about azurin purification), Will Wehbi (very knowledgeable about bioinorganic chemistry and a nice person), Angelo Di Bilio (very helpful and knowledgeable about everything related to azurin and I appreciate his help very much), Kristine Jensen (helped me a lot during my first summer and year at Caltech), Yen Nguyen (for many fun and crazy times during my first year), Jasmine Faraone-menella (an extremely nice and helpful person in general), Oliver Wenger (a nice and happy guy who has provided help with using the laser), Karn Sorasaene (the other Thai person in our group besides me who has been so nice and friendly, good luck at USC!), Steve Contakes (nice guy all around who has helped with nanosecond one measurements during my second year – best wishes at Azusa Pacific!), and Alex Dunn (a smart and nice guy all around who has

provided some good advice when I was searching for postdoc positions). I also thank Kyoko Fujita, Wendy Belliston-bittner, Shantanu Sharma, Libby Mayo, Pierre Kennepohl, Jenn Lee, Randy Villahermosa for also making this an interesting group. Each person listed has played some kind of role in my time here.

I thank Joe Drew, Mo Renteria, and Terry James, the stockroom guys (for all their help these past five years with bringing our needed chemicals and supplies and their help with the stockroom in general), Rick Gerhart (the talented glass blower who has helped fix many of my careless mistakes), and Larry Henling (the small molecule crystallographer who helped with obtaining a structure of a compound I made my first summer). I'll miss Dian Buchness and thank for her hard work. I like to think of her as the guardian angel of the Chemistry department's grad students before she left to start her new position in GPS. I also thank Pat Andersen, Catherine May, and Rick Jackson, Margot Hoyt, and Kathleen Hand for all the administrative help, and Laura Howe for her help these past several months with paperwork for graduation and exams. I also thank the wonderful staff in the Chemistry Department as well as in other departments for always being so helpful and friendly. People here are genuinely nice and want to help you out and I'm glad to have interacted with many. If I have forgotten anyone, I apologize.

I also thank my friends (too many to list here but you know who you are!) for providing support and friendship that I needed. I would like to thank Connie Lu for being supportive throughout my time here and for helping me with proofreading my prop. I think of her as a big sister.

I especially thank my mom, dad, and sister. My hard-working parents have sacrificed their lives for my sister and myself and provided unconditional love and care. I love them so much, and I would not have made it this far without them. My sister has been my best friend all my life and I love her dearly and thank her for all her advice and support. I know I always have my family to count on when times are rough. I thank my beloved dogs, Cotton and Frisky, who have both passed on. I still miss them, especially Cotton, for their friendship while growing up. I wished he could have lived for another few years for my wedding and for my graduation. Special thanks to the newest additions to my family, John, my new husband as well as his wonderful family who all have been supportive and caring.

The best outcome from these past five years is finding my best friend, soul-mate, and husband. I married the best person out there for me. John is the only person who can appreciate my quirkiness and sense of humor. There are no words to convey how much I love him. John has been a true and great supporter and has unconditionally loved me during my good and bad times. He has been non-judgmental of me and instrumental in instilling confidence. He has faith in me and my intellect even when I felt like digging hole and crawling into one because I didn't have faith in myself. These past several years have not been an easy ride, both academically and personally. I truly thank John for sticking by my side, even when I was irritable and depressed. I feel that what we both learned a lot about life and strengthened our commitment and determination to each other and to live life to the fullest.



*I dedicate this thesis to  
my family, my husband, John, and my beloved animals  
for their constant support and unconditional love.  
I love you all dearly.*

## ABSTRACT

The field of membrane protein folding is relatively new compared to soluble protein folding. This thesis describes spectroscopy investigations of the refolding and dynamics of a  $\beta$ -barrel membrane protein. The amphiphilic,  $\beta$ -barrel outer membrane protein A (OmpA) refolds and inserts directly into a lipid vesicle or micelle from a denatured state in aqueous urea solution. Spectroscopic probes used to study this system are native tryptophans located at positions 7, 15, 57, 102, and 143. Steady-state and time-resolved fluorescence measurements have been performed using single tryptophan mutants of full-length OmpA (325 residues) and the truncated, transmembrane domain (176 residues). Both full-length and truncated mutants exhibit similar tryptophan emission lifetimes, suggesting that the transmembrane microenvironment is not greatly perturbed by the presence of the C-terminus.

While the microenvironments of folded full-length and truncated OmpA appear similar, the dynamics of refolding at each tryptophan position exhibit subtle differences when the C-terminus is present. Specifically, we observe that tryptophan-102, which faces the pore interior, inserts and folds the fastest while tryptophan-7, which does not cross the bilayer, is the slowest. Fluorescence anisotropy decays also indicate that tryptophan-7 is the most flexible residue compared to the other tryptophans. Temperature studies below the lipid gel-liquid transition temperature have also been performed. In the lipid gel phase, OmpA adsorbs to the surface of the vesicles but contains immediate  $\beta$ -sheet structure upon folding as well as very hydrophobic tryptophan environments. It is still uncertain from ensemble measurements whether this species is a true intermediate.

Fluorescence energy transfer kinetics have successfully determined the intramolecular distance between tryptophan-7 and cysteine-175 labeled with a dansyl fluorophore. These results reveal that the barrel ends of OmpA come into contact early in the refolding process and remain close together up to the final assembly of the barrel. We also have evidence that the adsorbed species at low temperatures is not an intermediate in the folding pathway since no energy transfer is observed for this species. These spectroscopic investigations have provided the foundation for further fundamental studies to dissect the molecular mechanism of the folding pathway of OmpA as well as other integral membrane proteins.

## TABLE OF CONTENTS

Acknowledgements	iii
Abstract	x
Table of contents	xii
List of Figures	xiv
List of Tables	xxviii
<b>Chapter 1: Introduction to membrane protein folding</b>	<b>1</b>
1.1 Introduction	2
1.2 Thesis Overview	5
1.3 References	7
<b>Chapter 2: Preparation of OmpA proteins and phospholipids vesicles</b>	<b>9</b>
2.1 Introduction	10
2.2 Materials and Methods	24
2.3 Results and Discussion	30
2.4 Conclusions	38
2.5 References	39
<b>Chapter 3: Probing folded and unfolded states of OmpA tryptophan mutants using steady-state and time-resolved tryptophan fluorescence</b>	<b>44</b>
3.1 Introduction	45
3.2 Experimentals	49
3.3 Results and Discussion	53
3.4 Conclusions	65
3.5 References	99

<b>Chapter 4: Tryptophan fluorescence quenching by brominated lipids</b>	<b>102</b>
4.1 Introduction	103
4.2 Experimentals	106
4.3 Results and Discussion	106
4.4 Conclusions	119
4.5 References	120
<b>Chapter 5: Investigations of the C-terminal domain on the refolding of OmpA tryptophan mutants using steady-state fluorescence and circular dichroism spectroscopy</b>	<b>121</b>
5.1 Introduction	122
5.2 Experimentals	130
5.3 Results and Discussion	131
5.4 Conclusions	160
5.5 References	161
<b>Chapter 6: Fluorescence energy transfer kinetics of full-length and truncated OmpA W7 mutants</b>	<b>163</b>
6.1 Introduction	164
6.2 Experimentals	170
6.3 Results and Discussion	173
6.4 Conclusions	195
6.5 References	196
<b>Chapter 7: Thesis summary and perspectives</b>	<b>198</b>
References	203

## LIST OF FIGURES

- Figure 2.1.** Schematic of the two-stage model proposed for general folding of  $\alpha$ -helical bundles (top) and the concerted model for the folding of  $\beta$ -barrels into the lipid bilayer. 11
- Figure 2.2.** Schematic illustrating the general cell envelope of *E.coli*. 14  
The inner membrane (IM) is separated from the outer membrane (OM) by the aqueous periplasm, which contains the peptidoglycan cell wall component. Inner membrane proteins contain  $\alpha$ -helical domains while outer membrane proteins contain  $\beta$ -barrel transmembrane domains. Both the IM and OM contain lipoproteins that are attached to their periplasmic sides. Adapted from Ruiz et al., 2006.
- Figure 2.3.** The amino acid sequence of wt-OmpA is shown. The signal sequence prior to the OmpA sequence is shown in parentheses. Native Trp (W7, W15, W57, W102, W143) are highlighted in blue. The last residue in all truncated proteins is highlighted in red. A175 is shown in green and C290 and C302 that were mutated to serines are shown in orange. 20
- Figure 2.4.** Structure of the OmpA transmembrane domain (residues 1-171), solved by X-ray crystallography (Pautsch & Schulz, 1998). The 5 native Trp are shown along with the approximate dimensions and an illustration of the C-terminal tail in the periplasmic space. The approximate location of the transmembrane region is shown with the red, dashed lines. 21

<b>Figure 2.5.</b> Schematic of the oriented insertion of OmpA into the lipid vesicles in refolding <i>in vitro</i> experiments. The C-terminus tail of OmpA is located on the exterior of the vesicle while the extracellular loops are on the interior of the vesicle.	22
<b>Figure 2.6.</b> Cross section of the OmpA transmembrane structure displaying the Trp orientations. W102 is the only Trp that faces the OmpA pore. The other 4 Trp face the exterior of the bilayer and interact with the lipid bilayer.	23
<b>Figure 2.7.</b> Typical DLS scan showing the diameter of DMPC vesicles. Sizes range from 20-60 nm in diameter.	33
<b>Figure 2.8.</b> Scheme showing the major steps of OmpA extraction from outer membranes.	34
<b>Figure 2.9.</b> Representative FPLC trace for purification of OmpA mutants on a 35 HiTrap QFF column. A 0-200 mM NaCl gradient was used to elute unfolded protein, which comes out as a broad peak on the trace.	35
<b>Figure 2.10.</b> Typical SDS-PAGE of FPLC purified OmpA is shown on the left. The right figure shows unfolded (35 kDa) and folded (30 kDa) OmpA in vesicles.	36
<b>Figure 3.1.</b> Structures of OG detergent and DMPC phospholipid. Illustrations of a detergent micelle and unilamellar vesicles are shown, along with approximate sizes.	48
<b>Figure 3.2.</b> Schematic of the setup for time-resolved measurements using	52

the femtosecond Titanium:sapphire (Ti:Sap) laser and the picosecond streak camera. Not all optical parts are illustrated. Figure not drawn to scale. Abbreviation PD = photodiode.

**Figure 3.3.** CD spectra of wild-type, full-length, and truncated Trp mutants unfolded in urea (top) and buffer (bottom). 66

**Figure 3.4.** CD spectra of wild-type, full-length, and truncated Trp mutants folded in OG micelles (top), DMPC vesicles at 30 °C (middle), and DMPC vesicles at 15 °C (bottom). 67

**Figure 3.5.** Overlay of CD spectra for Trp mutants at 30 °C (solid) and 15°C (dotted). Truncated mutants display lower  $\beta$ -sheet signal than full-length. 15 °C data were averaged over the last 30-60 min of refolding. 30 °C data were averaged over 130-150 min into folding. 68

**Figure 3.6.** Steady-state fluorescence of NATA in urea, phosphate buffer, OG micelles, and DMPC vesicles at 30 °C. Spectra at 15 °C have the same emission maxima at 352 nm as the 30 °C spectra. 69

**Figure 3.7.** Steady-state fluorescence spectra of full-length (solid lines) and truncated (dotted lines) OmpA mutants unfolded in urea at 30 °C. Spectra were corrected for vesicle-only background and normalized to protein concentration. 70

**Figure 3.8.** Steady-state fluorescence spectra of full-length (solid lines) and truncated (dotted lines) OmpA mutants folded in OG micelles at 30 °C. Spectra were corrected for vesicle-only background and normalized to protein concentration. 71



<b>Figure 3.9.</b> Steady-state fluorescence spectra of full-length (solid lines) and truncated OmpA mutants folded in DMPC vesicles at 30 °C. Spectra were corrected for vesicle-only background and normalized to protein concentration.	72
<b>Figure 3.10.</b> Steady-state fluorescence spectra of full-length (solid lines) and truncated (dotted lines) OmpA mutants folded in DMPC vesicles at 15 °C. Spectra were corrected for vesicle-only background and normalized to protein concentration.	73
<b>Figure 3.11.</b> Comparison of steady-state fluorescence spectra of full-length and truncated OmpA mutants folded in DMPC vesicles at 30 °C (solid lines) and 15 °C (dotted lines). Top panel shows full-length mutants at both temperatures. Bottom panel shows truncated mutants at both temperatures. Spectra were corrected for vesicle-only background and normalized to protein concentration.	74
<b>Figure 3.12.</b> Steady-state fluorescence spectra of full-length (solid lines) and truncated (dotted lines) OmpA mutants unfolded in phosphate buffer at 30 °C. Spectra were corrected for vesicle-only background and normalized to protein concentration.	75
<b>Figure 3.13</b> Time-resolved fluorescence of NATA in urea, phosphate buffer, micelles, and vesicles (30 °C and 15 °C).	77
<b>Figure 3.14.</b> Time-resolved fluorescence of Trp mutants in urea.	79
<b>Figure 3.15.</b> Time-resolved fluorescence of Trp mutants in OG micelles.	81
<b>Figure 3.16.</b> Time-resolved fluorescence of Trp mutants in DMPC	83

vesicles, 30 °C.

<b>Figure 3.17.</b> Fluorescence decays of full-length (left) and truncated mutants (right), mutants unfolded in urea (black), folded in OG micelles	85
<b>Figure 3.18.</b> Time-resolved fluorescence of Trp mutants in DMPC vesicles, 15 °C	86
<b>Figure 3.19.</b> Steady-state anisotropy of mutants in urea.	89
<b>Figure 3.20.</b> Steady-state anisotropy of mutants in micelles.	90
<b>Figure 3.21.</b> Steady-state anisotropy of mutants in DMPC.	91
<b>Figure 3.22.</b> Time-resolved anisotropy of full-length (top) and truncated mutants (bottom) unfolded in urea. Measurements were taken in a 50 ns time window.	93
<b>Figure 3.23.</b> Time-resolved anisotropy of full-length (top) and truncated mutants (bottom) folded in OG micelles. Measurements were taken in a 50 ns time window.	94
<b>Figure 3.24.</b> Time-resolved anisotropy of full-length (top) and truncated mutants (bottom) folded in DMPC vesicles at 30 °C. Measurements were taken in a 50 ns time window.	95
<b>Figure 3.25.</b> Overlay of anisotropy decays for full-length and truncated mutants for each Trp position.	96
<b>Figure 3.26.</b> Time-resolved anisotropy of full-length (top) and truncated mutants (bottom) folded in DMPC vesicles at 30 °C. Measurements were taken in a 5 ns time window.	97

<b>Figure 4.1.</b> Structures of DMPC, 1-palmitoyl-2-stearoyl (6-7) dibromo- <i>sn</i> -glycero-3-phosphocholine (6,7-DiBr), and 1-palmitoyl-2-stearoyl (11-12) dibromo- <i>sn</i> -glycero-3-phosphocholine (11,12-DiBr). Mixed vesicles of DMPC/6,7-DiBr and DMPC/11,12-DiBr were prepared with a 0.25 molar fraction of DMPC:DiBr lipids.	108
<b>Figure 4.2.</b> Steady-state fluorescence of full-length (top) and truncated (bottom) mutants in DMPC (solid lines) and 6,7-DiBr (dashed lines) vesicles	113
<b>Figure 4.3.</b> Steady-state fluorescence of full-length (top) and truncated (bottom) mutants in DMPC (solid lines) and 11,12-DiBr (dashed lines) vesicles	114
<b>Figure 4.4.</b> Fluorescence decays of full-length (top) and truncated (bottom) Trp mutants folded in DMPC vesicles (solid lines) and 6,7-DiBr vesicles (dashed lines) at 30 °C.	115
<b>Figure 4.5.</b> Fluorescence decays of full-length (top) and truncated (bottom) Trp mutants folded in DMPC vesicles (solid lines) and 11,12-DiBr vesicles (dashed lines) at 30 °C.	116
<b>Figure 4.6.</b> Fluorescence quenching rates of full-length (top) and truncated (bottom) mutants in 6,7-DiBr vesicles at 30 °C.	117
<b>Figure 4.7.</b> Fluorescence quenching rates of full-length (top) and truncated (bottom) mutants in 11,12-DiBr vesicles at 30 °C.	118
<b>Figure 4.8.</b> Overlay of the quenching rate of full-length mutants (left) and truncated mutants (right) folded in the two different DiBr lipid positions.	119

- Figure 4.9.** Overlay of the quenching rates of full-length mutants (red) and truncated mutants (blue) folded in 6,7-DiBr (left) and 11,12-DiBr (right). 120
- Figure 5.1.** Schematic of the current model of OmpA folding into the lipid bilayer. The chart indicates the average distances of the Trp residues from the center of the bilayer for each intermediate and the native structure. Adapted from Kleinschmidt, 2003. 132
- Figure 5.2.** Fluorescence spectra of W143t immediately following greater than 120 fold dilution of 8 M urea into phosphate buffer (KPi). During the 120 minute reaction, the spectra showed no systematic shifts. 144
- Figure 5.3.** Fluorescence spectra of full-length W7 mutants immediately following protein injection to initiate folding into DMPC vesicles at 30 °C. During the 120 minute folding reaction, general changes in the spectra are observed in the form of a blue-shift in emission maximum and an increase in quantum yield. 145
- Figure 5.4.** Fluorescence spectra of W7t immediately following protein injection to initiate folding into DMPC vesicles at 30 °C. During the 120 minute folding reaction, general changes in the spectra are observed in the form of a blue-shift in emission maximum and an increase in quantum yield. 146
- Figure 5.5.** Relative changes in emission maxima (top) and emission intensity (bottom) as a function of folding time. A value of “1” indicates the final emission maximum or intensity at  $t = 120$  minutes. 147

<b>Figure 5.6.</b> Comparison of the rate of blue-shifting and quantum yield increase for W7 and W7t. Dotted line indicates the approximate time when blue-shift is complete while quantum yield continues to increase.	148
<b>Figure 5.7.</b> Comparison of the rate of blue-shifting and quantum yield increase for W15 and W15t. Dotted line indicates the approximate time when blue-shift is complete while quantum yield continues to increase.	149
<b>Figure 5.8.</b> Comparison of the rate of blue-shifting and quantum yield increase for W57 and W57t. Dotted line indicates the approximate time when blue-shift is complete while quantum yield continues to increase.	150
<b>Figure 5.9.</b> Comparison of the rate of blue-shifting and quantum yield increase for W102 and W102t. Dotted line indicates the approximate time when blue-shift is complete while quantum yield continues to increase.	151
<b>Figure 5.10.</b> Comparison of the rate of blue-shifting and quantum yield increase for W143 and W143t. Dotted line indicates the approximate time when blue-shift is complete while quantum yield continues to increase.	152
<b>Figure 5.11.</b> Fluorescence intensity of Trp mutants monitored at 330 nm immediately following initiation of folding reaction in DMPC for full-length mutants. Kinetic traces were normalized to have equivalent maximum emission intensities at 120 minutes.	153
<b>Figure 5.12.</b> Fluorescence intensity of Trp mutants monitored at 330 nm	154

immediately following initiation of folding reaction in DMPC for truncated mutants. Kinetic traces were normalized to have equivalent maximum emission intensities at 120 minutes.

**Figure 5.13.** Overlay of fluorescence intensity at 330 nm for full-length and truncated mutants at each Trp position. 155

**Figure 5.14.** Fluorescence spectra (top) of W7t immediately following protein injection to initiate folding into DMPC vesicles at 15 °C. The intensity at 330 nm is shown on the bottom. Spectra are immediately blue-shifted upon addition of protein to the cold vesicles. During the 60 minutes of data collection, no changes in the spectra and 330 nm values are observed. 156

**Figure 5.15.** Fluorescence spectra (top) of W15t immediately following protein injection to initiate folding into DMPC vesicles at 15 °C. The intensity at 330 nm is shown on the bottom. Spectra are immediately blue-shifted upon addition of protein to the cold vesicles. During the 60 minutes of data collection, no changes in the spectra and 330 nm values are observed. 157

**Figure 5.16.** Fluorescence spectra (top) of W102t immediately following protein injection to initiate folding into DMPC vesicles at 15 °C. The intensity at 330 nm is shown on the bottom. Spectra are immediately blue-shifted upon addition of protein to the cold vesicles. During the 60 minutes of data collection, very small changes in the spectra and 330 nm values are observed. 158

- Figure 5.17.** Fluorescence intensity measured at 330 nm for all Trp mutants immediately following protein injection to initiate adsorption onto DMPC vesicles at 15 °C. During the 60 minutes of data collection, no changes in the 330 nm values are observed. 159
- Figure 5.18.** CD spectra of full-length Trp mutants immediately following initiation of a folding reaction in 30 °C DMPC (left) and 15 °C DMPC (right). The time scales for folding are different for 30 °C and 15 °C samples. As the protein refolds, the CD spectra evolved to form  $\beta$ -sheet signal for folding at 30 °C. In contrast, no changes in signal were observed for refolding at 15 °C. 160
- Figure 5.19.** CD spectra of truncated Trp mutants immediately following initiation of a folding reaction in 30 °C DMPC (left) and 15 °C DMPC (right). The time scales for folding are different for 30 °C and 15 °C samples. As the protein refolds, the CD spectra evolved to form  $\beta$ -sheet signal for folding at 30 °C. In contrast, no changes in signal were observed for refolding at 15 °C. 161
- Figure 5.20.** Top panel shows the molar ellipticity at 206 nm for full-length mutants as the proteins fold into DMPC vesicles at 30 °C. Bottom panel shows the molar ellipticity at 206 nm for truncated mutants as the proteins fold into DMPC vesicles at 30 °C. 162
- Figure 5.21.** Changes in molar ellipticity at 206 nm for full-length mutants as the proteins fold into DMPC vesicles at 30 °C. Blue traces are truncated mutants and red traces are full-length mutants. 163

**Figure 6.1.** Sample potential energy landscape for lysozyme folding. 168

Adapted from Dobson et al., 1998.

**Figure 6.2.** Schematic depicting the relationship between protein 173

conformations and fluorescence decay kinetics. The left side shows a simplified energy landscape funnel. At the top of the funnel, an ensemble of unfolded proteins will exhibit a broad distribution of distances ( $P(r)$ ) between the FET donors and acceptors and slow excited-decay kinetics. At the bottom, an ensemble of folded proteins should exhibit a narrow distance distribution and faster excited-state decay kinetics. The distance distribution function can be transformed using Eq. 1 to a distribution of fluorescence decay rates ( $k$ ).  $P(k)$  can be transformed using Eq. 4 to a fluorescence decay intensity profile ( $I(t)$ ). Figure obtained from Julia Lyubovitsky's dissertation (Lyubovitsky, 2003).

**Figure 6.3.** Overlap of NATA emission with normalized Dns absorption. 182

**Figure 6.4.** Reaction of a general cysteine with 1,5 IEADANS to produce 184

the dansylated cysteine on the protein. Note that cysteine was drawn as a free amino acid for simplicity. In reality, these cysteines are attached to the protein.

**Figure 6.5.** Structure of OmpA showing the positions and distance of W7 185

and A175C. The  $\alpha$ -carbon position of W7  $\sim 16$  Å from to A175C, according to the NMR structure (PDB file IG90).

**Figure 6.6.** Absorption spectra of time points from a side-by-side labeling 186



reaction of W7/A175C and the control protein, W7/C290S/C302S (abbreviated as W7/0C), with IAEDANS. The ratio of Dns to protein indicates that 5 hr is sufficient for labeling.

**Figure 6.7.** Fluorescence spectra of full-length W7/A175C-Dns 187

immediately following protein injection to initiate folding into DMPC vesicles at 30°C. Two general processes are observed (top): blue-shift in emission maxima and quantum yield increase. Relative changes in emission maxima (bottom, blue trace) and emission intensity (bottom, green and red traces) are shown as a function of folding time. Traces were normalized so that a value of “1” corresponds to the emission maximum or intensity at  $t = 2$  hr.

**Figure 6.8.** Fluorescence spectra of truncated W7t/A175C-Dns 188

immediately following protein injection to initiate folding into DMPC vesicles at 30 °C. Two general processes are observed (top): blue-shift in emission maxima and quantum yield increase. Relative changes in emission maxima (bottom, blue trace) and emission intensity (bottom, green and red traces) are shown as a function of folding time. Traces were normalized so that a value of “1” corresponds to the emission maximum or intensity at  $t = 2$  hr.

**Figure 6.9.** Excitation of Dns in W7/A175C-Dns with 340 nm excitation 189

does not produce a continuous rise in emission.

**Figure 6.10.** Fluorescence spectra of W7/A175C (unlabeled) immediately 190

following protein injection to initiate folding into DMPC vesicles at 30°C.

Relative changes in emission maxima (bottom, blue trace) and emission intensity (bottom, red trace) are shown as a function of folding time.

Traces were normalized so that a value of “1” corresponds to the emission maximum or intensity at  $t = 2$  hr.

**Figure 6.11.** Fluorescence spectra of W7t/A175C (unlabeled) 191

immediately following protein injection to initiate folding into DMPC vesicles at 30°C. Relative changes in emission maxima (bottom, blue trace) and emission intensity (bottom, red trace) are shown as a function of folding time. Traces were normalized so that a value of “1” corresponds to the emission maximum or intensity at  $t = 2$  hr.

**Figure 6. 12.** Energy transfer rates are shown for the different folding 192

times for W7/A175C-Dns and W7t/A175C-Dns. The energy transfer rate has decayed to a constant by  $\sim 14$  min for W7/A175C and between 10-60 min for W7t/A175C.

**Figure 6. 13.** Typical data sets collected for FET kinetics. Top, left graph 193

are measurements of Trp decays as the protein folds into DMPC vesicles;

Trp decays become only slightly faster as the protein folds. Top, right

graph are measurements of Dns emission using 290 nm excitation; energy

transfer is observed as a slow rise in intensity. Bottom graph is Dns

emission from W7/A175C-Dns in urea; no energy transfer to Dns is

observed.

**Figure 6.14.** CD spectra of W7/A175C, W7t/A175C, and wild-type 198

OmpA. Note that the ellipticities are lower than those from Chapter 3, most likely due to inaccurate protein concentrations used to determine molar ellipticities.

## LIST OF TABLES

<b>Table 2.1.</b> List of proteins prepared and their number of residues, calculated molecular weight (kDa), and calculated extinction coefficients.	37
<b>Table 3.1</b> List of emission maxima for the different Trp mutants in urea, OG micelles, and DMPC vesicles in nm.	76
<b>Table 3.2.</b> Exponential (mono-, bi-, tri-) fits of lifetimes of NATA in urea, phosphate buffer, micelles, and vesicles (30 °C and 15 °C). Tryptophan decays were fit with triple exponentials. Amplitudes (amp) and their corresponding lifetimes ( $\tau$ ) are shown as well as the amplitude weighted lifetimes.	78
<b>Table 3.3.</b> Lifetimes of full-length and truncated mutants unfolded in urea. Tryptophan decays were fit to biexponentials or triple exponentials. Amplitudes (amp) and their corresponding lifetimes ( $\tau$ ) are shown as well as the amplitude weighted lifetimes.	80
<b>Table 3.4.</b> Lifetimes of full-length and truncated mutants folded in OG micelles. Tryptophan decays were fit to triple exponentials. Amplitudes (amp) and their corresponding lifetimes ( $\tau$ ) are shown as well as the weighted lifetimes.	82
<b>Table 3.5.</b> Lifetimes of full-length and truncated mutants folded in DMPC vesicles at 30 °C. Tryptophan decays were fit to biexponentials or triple exponentials. Amplitudes (amp) and their corresponding lifetimes ( $\tau$ ) are shown as well as the weighted lifetimes.	84

<b>Table 3.6.</b> Lifetimes of full-length and truncated mutants folded in DMPC vesicles at 15 °C. Tryptophan decays were fitted to biexponentials. Amplitudes (amp) and their corresponding lifetimes ( $\tau$ ) are shown as well as the weighted lifetimes.	87
<b>Table 3.7.</b> List summarizing the amplitude weighted lifetimes of NATA and Trp mutants in urea, micelles, and vesicles.	88
<b>Table 3.8.</b> Steady-state anisotropy of NATA and Trp mutants in urea, OG micelles, and DMPC vesicles (30°C).	92
<b>Table 3.9.</b> Average slow and fast correlation times ( $\Theta$ ) for both full-length and truncated mutants.	98
<b>Table 4.1.</b> Ratios of quenched (F) to unquenched ( $F_0$ ) emission maxima for 6,7-DiBr and 11,12-DiBr. The quenching rates (ratio of quenched to unquenched fluorescence decays) shown are amplitude weighted average lifetimes from biexponential fits ( $y = c_0 + ae^{-k_1t} + be^{-k_2t}$ ). The unquenched fractions ( $c_0$ ) are also listed.	121
<b>Table 6.1.</b> Lifetimes and amplitudes of the Dns excited-state decay	183
<b>Table 6.2.</b> W7/A175C folding into DMPC vesicles at 30 °C. Probability weighted energy transfer rates ( $k_{et}$ ) and their corresponding weighted distances ( $r$ ). The percent of unquenched fluorescence is also listed.	194
<b>Table 6.3.</b> Percentage of unquenched Trp fluorescence for W7/A175C folding into DMPC vesicles at 15°C.	194
<b>Table 6.4.</b> W7t/A175C folding into DMPC vesicles at 30°C. Probability	195

weighted energy transfer rates ( $k_{et}$ ) and their corresponding weighted distances ( $r$ ). The percent of unquenched fluorescence is also listed.

**Table 6.5.** Percentage of unquenched Trp fluorescence for W7t/A175C folding into DMPC vesicles at 15°C. 195

**Table 6.6.** W7/A175C folding into OG micelles at 30°C. Probability weighted energy transfer rates ( $k_{et}$ ) and their corresponding weighted distances ( $r$ ). The percent of unquenched fluorescence is also listed. 196

**Table 6.7.** W7/A175C folding into OG micelles at 15°C. Probability weighted energy transfer rates ( $k_{et}$ ) and their corresponding weighted distances ( $r$ ). The percent of unquenched fluorescence is also listed. 196

**Table 6.8.** W7t/A175C folding into OG micelles at 30°C. Probability weighted energy transfer rates ( $k_{et}$ ) and their corresponding weighted distances ( $r$ ). The percent of unquenched fluorescence is also listed. 197

**Table 6.9.** W7t/A175C folding into OG micelles at 15°C. Probability weighted energy transfer rates ( $k_{et}$ ) and their corresponding weighted distances ( $r$ ). The percent of unquenched fluorescence is also listed. 197